SPECIAL ISSUE PAPER

WILEY

Geomorphically mediated carbon dynamics of floodplain soils and implications for net effect of carbon erosion

Timothy A. Quine[1] | Elizabeth L. Cressey[1] | Jennifer A. J. Dungait[1] |
Sarah De Baets[1,2,3] | Jeroen Meersmans[1,2,4] | Matthew W. Jones[1,5] |
Andrew P. Nicholas[1]

[1]Geography, College of Life & Environmental Sciences, University of Exeter, Exeter, UK

[2]Soil and Agrifood Institute, Cranfield University, Cranfield, UK

[3]Research Coordination Office, KU Leuven, Leuven, Belgium

[4]TERRA Teaching and Research Centre, Gembloux Agro-Bio Tech, University of Liège, Gembloux, Belgium

[5]Tyndall Centre for Climate Change Research, School of Environmental Sciences, University of East Anglia, Norwich Research Park, Norwich, UK

Correspondence
Timothy A. Quine, College of Life and Environmental Sciences, University of Exeter, Exeter EX4 4QL, UK.
Email: t.a.quine@exeter.ac.uk

Abstract

The fate of organic carbon deposited in floodplain sediments is an important control on the magnitude and direction of the carbon flux from anthropogenically accelerated erosion and channelization of the riverine network. Globally, carbon deposition rates and mean residence time (MRT) within different geomorphic settings remains poorly constrained. We sampled soil profiles to 0.8 m depth from two geomorphic zones: active channel belt (ACB) and lowland floodplain, under long-term pasture adjacent to the river Culm in SW England, UK. We evaluated sedimentation rates and carbon storage using fallout radionuclide ^{137}Cs, particle size and total carbon analyses. Variation in decomposition was assessed via empirical (soil aggregate size, density fractionation combined with natural abundance ^{13}C analysis) and modelling simulation (using the RothC model and catchment implications explored using a floodplain evolution model). Sedimentation and carbon accumulation rates were 5–6 times greater in the ACB than the floodplain. Carbon decomposition rates also varied with geomorphic setting. In floodplain cores, faster decomposition rates were indicated by greater ^{13}C-enrichment and subsoils dominated by mineral-associated soil organic carbon. Whereas, in the ACB, carbon was less processed and ^{13}C-depleted, with light fraction and macroaggregate-carbon throughout the cores, and RothC modelled decomposition rates were 4-fold less than lowland floodplain cores. Including the ACB in floodplain carbon MRT calculations increased overall MRT by 10%. The major differences in the balance of sedimentation and decomposition rates between active and inactive floodplains suggests the relative extent of these contrasting zones is critical to the overall carbon balance. Restoration projects could enhance soil carbon storage by maximizing active floodplain areas by increasing river channel complexity.

KEYWORDS
carbon dynamics, carbon storage, erosion, floodplain, mean residence time, sedimentation, source/sink, stable isotopes

1 | INTRODUCTION

Floodplains cover less than 1% of the global land surface but account for up to 8% of soil organic carbon (SOC) storage (D'Elia et al., 2017; Sutfin et al., 2016). The dynamic riparian zone acts as a buffer between aquatic ecosystems and upland landscapes; lateral deposition retains sediment and carbon in the landscape, and is recognized as an important flux in the global carbon cycle erosion debate (D'Elia et al., 2017; Regnier et al., 2013; Ricker et al., 2012; Sutfin et al., 2016; Sutfin et al., 2021). Inventories report carbon in depositional soils can be protected from loss on 50 y timescales (Aufdenkampe et al., 2011; Wang et al., 2014; Wohl et al., 2017), but the mechanisms controlling inputs or loss from this important carbon pool are not well-defined. Riparian systems are estimated to receive 2.3–2.9 Pg C y^{-1} (Glendell et al., 2018; Regnier et al., 2013; Wohl et al., 2017). Sutfin et al. (2016) reported ~22% of carbon entering headwater streams is unaccounted for after quantifying delivery to oceans or losses to outgassing as carbon dioxide (CO_2), suggesting there is a substantial reservoir of carbon in riparian systems derived from sediment deposition. To quantify the landscape-scale impact of erosion, it is essential to understand the transfers and carbon dynamics of downstream intermediate storage environments (e.g., floodplains, wetlands, and lakes; Scheingross et al., 2021).

Floodplains are characterized by a high degree of geomorphic and hydrologic complexity, with an active channel, geomorphic floodplain, hyporheic aquifer, and associated riverine wetlands, and feature a diverse range of sedimentation mechanisms (Lewin et al., 2017; Nanson & Croke, 1992; Wohl et al., 2021). The river corridor can occupy an entire valley floor or be limited naturally or anthropogenically (i.e., weirs, levees, and bridge construction; Wohl et al., 2021). In the broadest terms, floodplain sediments can be separated into channel deposits (e.g., associated with bar formation during channel migration; Nanson, 1980) and over-bank deposits (e.g., typically fine-grained sediments deposited at rates declining with distance from the main river channel; Pizzuto, 1987). Importantly, channel migration also reworks floodplain sediments and drives local changes in river sinuosity resulting in bend abandonment by cutoff (Constantine & Dunne, 2008). Consequently, these processes are responsible for both the storage and remobilisation of sediment (and associated carbon), and the evolution of floodplain topographic relief (Lewin & Ashworth, 2014), which generally scales with channel depth. Therefore, localized geomorphology and valley geometry are important factors explaining the variability in sediment residence time, with younger deposits being more vulnerable to reworking; wide valleys with low energy river flow are more likely to accumulate sediment during flood events (Sutfin & Wohl, 2019). Annual variation in river water level also scale with river depth and floodplains are typically characterized by a diverse range of hydrological environments, in terms of inundation frequency and soil moisture content, with connectivity and complexity increasing with wetness (Wohl et al., 2021). Wetter soils tend to have greater SOC content, wetlands can be older and more stable with slower decomposition, whilst dry, drained floodplains can be hydrologically disconnected with rapid decomposition and be a source of carbon (Lininger et al., 2018; Wohl et al., 2021).

Under natural conditions, floodplains are a resilient, dynamically stable system between water, sediment and biota; dynamically adjusted through deposition, sedimentation, erosion, exchange and transport (Wohl et al., 2021). 50%–90% of European wetland ecosystems have been lost and more than 80% of the remaining floodplain wetlands significantly altered (Wohl et al., 2021). Following agricultural land use change, forest clearance and beaver eradication, overbank silt-clay sedimentation has transformed European floodplains over the past 4000–2000 y, covering former wetlands and hydric soils, silting secondary channels, and changing anabranching channels to single incised meandering channels in flat inorganic floodplains (Brown et al., 2018). Globally, soil erosion and sedimentation have accelerated over the past 200 y with the industrial use of rivers and intensive agricultural practices (Brown et al., 2018; Ricker et al., 2012; Wohl et al., 2021). This sedimentation can result in a diverse vertical structure, with buried horizons containing large carbon contents comparable to surface soil layers (Chaopricha & Marín-Spiotta, 2014; Doetterl et al., 2013; Mayer et al., 2018; Wohl et al., 2017). Burial of eroded soils removes carbon from actively cycling topsoil to the subsoil, where decomposition occurs at a slower rate, offering a potential net carbon sink (Lal, 2019; Van Oost et al., 2012; Wang et al., 2014), and prolonged waterlogging in regularly inundated floodplain soils can further reduce decomposition rates (D'Elia et al., 2017; Doetterl et al., 2013; Mayer et al., 2018). Conversely, rapid mineralization of catchment-derived biologically-available SOC in moist floodplain soils may offset these sequestering mechanisms, driving the erosion cascade towards steady-state or net source (Lugato et al., 2018; Ni et al., 2012; Rosenbloom et al., 2006; Wohl et al., 2017).

The fate of transported SOC, deposited in different depositional environments within riverine networks, remains poorly constrained with storage varying spatially and temporally (Doetterl et al., 2013; Graf-Rosenfellner et al., 2016; Lal, 2019; Wohl et al., 2017). The potential for floodplain carbon storage is complex and highly variable: first, through geometry, which can control sediment residence time, water table, soil texture, carbon input; and second, hydrological connectivity impacting on preservation through environmental controls on carbon stability (Berhe & Kleber, 2013; Doetterl et al., 2013; Hinshaw & Wohl, 2021; Lininger et al., 2018; Scheingross et al., 2021; Sutfin et al., 2021). Deposited bare sediment surfaces can accumulate carbon inputs from autochthonous vegetation; the residence time of this sediment is key, accumulated carbon can subsequently be eroded and transported downstream or mineralised (Lininger et al., 2018). Extremely variable floodplain carbon accumulation rates of 0.03–12.2 Mg C ha^{-1} y^{-1} alongside stock estimates of 1.4–>1000 Mg C ha^{-1} have been reported, caused by site specific climate, geology, morphology—channel and valley, and river flow, even within a single river system (Hinshaw & Wohl, 2021; Sutfin et al., 2016). However, these studies have not related actual carbon stocks in floodplains to the turnover rates of originally deposited carbon to allow full budgeting to be undertaken (Rosenbloom et al., 2006; Sutfin et al., 2016).

In this paper, we aim to advance the understanding of this vital component of the sediment cascade within the land-ocean aquatic continuum (Regnier et al., 2013), and address the key question in this

context: "does the extent to which lowland temperate floodplain environments act as a net sink or source of carbon vary according to its geomorphic context?" Specifically, we examine two well-defined geomorphic zones (i.e., the Active Channel Belt (ACB) and lowland floodplain) utilizing a combined empirical assessment and modelling study of a "typical" lowland managed floodplain in SW England to test the following hypotheses:

1. The ACB has greater storage and preservation potential for catchment-derived carbon compared to the lowland floodplain;
2. The mean residence time (MRT) of catchment-derived carbon is determined by its distribution between the ACB and floodplain and the associated decomposition rate of each geomorphic context;
3. Net exchange of carbon to the atmosphere is determined by its MRT and by the duration of sediment residence in the ACB.

2 | MATERIALS AND METHODS

2.1 | Site selection and sampling

Two well-defined lowland geomorphic zones adjacent to the river Culm in SW England, UK (Figure 1; Walling et al., 2006) were examined as a case study to parameterise the model pools and fluxes, namely: infrequently flooded, relatively high elevation floodplain surface (aerobic for most of the year) in the lowland floodplain; and frequently waterlogged former channels of the river (cutoffs, i.e., the ACB). The river Culm catchment, of 226 km^2, has predominantly loamy-clayey acidic floodplain soils (mean soil core pH < 5.9), consisting of alluvial gleys, with loamy brown earth bordering the floodplain. 24.5% of the catchment area consists of alluvium over Permian Breccia and sandstone (Hooke, 1977). The predominantly impervious catchment bedrock can result in a flashy response to high precipitation and high flood discharge (Bennett et al., 2011). Selected catchment properties are detailed in Table 1. The area of ACB was estimated to be 0.02 km^2, following catchment digitization, <0.01% of the total catchment. The Culm is a meandering river, with a shallow channel over a gravel bed flowing in a wide floodplain (up to 800 m in width; Hooke, 1977). The catchment has undergone extensive changes from its natural condition to the present day, with evidence of human activity since the Mesolithic period, since the 1800s pastural land use has dominated the lowland Culm (i.e., summer livestock grazing or hay production; Bennett et al., 2011; Hooke, 1977). Mills were recorded on the Culm since the Domesday book in 1086 until the mid-19th century, resulting in a heavily managed water flow straightening the channel (Hooke, 1977). During the mid-19th century, weirs and mill channels fell into disrepair and most remaining were destroyed by flooding in the 1960s resulting in a return to a meandering river form. UK agricultural policies in the 1960s encouraged drainage and hedge removal resulting in increased channel flow, peakiness and meandering (Hooke, 1977).

Here, we first consolidated multiple lines of previously unpublished observational data to evidence potential carbon storage and

second simulated floodplain carbon storage and sediment retention. To this end, we characterized the nature of sediments deposited during overbank flood events, a total of 39 surface sediment samples were collected after Spring and Autumn inundation events on the Culm floodplain in March (n = 31) and September (n = 8) of 2008. As in Graf-Rosenfellner et al. (2016), sediment samples were collected using surface scrapes of the top 5 mm of sediment from the floodplain surface. Freshly deposited samples were taken with a trowel directly after a sedimentation event. All surface sediment samples were stored in plastic bags at 4°C and processed within 48 h of sampling. Data from the two inundation events were analysed together to estimate the average total carbon input to the soils from sedimentation.

To characterize carbon depth distribution in a UK grassland floodplain, soil profiles located in the two geomorphic zones were sampled. Three preliminary soil cores were collected in March 2008—two sediment cores were extracted from the ACB in rapidly infilling cut-offs, which had been excised from the main channel (110 mm diameter) to a depth of 0.8 m using a percussion hammer (Wacker BH23, Wacker Neuson Ltd, UK; ACB-1 (1) and ACB-2 (1); Figure 1); and one core was extracted from the floodplain zone at Smithincott within 2 m elevation of the main channel (F-1 (1); Figure 1). After extraction, cores were sealed in 1 m sections in plastic tubes and stored at 4°C until analysis. An additional 7 cores from Smithincott (ACB-3 (2), F-2:7 (2); Figure 1) and 4 from Rewe (F-8:11 (2); Figure 1; maximum depth 0.8 m or to the bedload) were extracted in October 2008 following summer flooding to further evaluate carbon spatial distribution and the proposed carbon decay model. As sediment carbon dynamics are active over decadal timescales, data from cores sampled on different dates in 2008 were composited (Zimmermann et al., 2007).

2.2 | Empirical assessment of carbon storage in the ACB and floodplain

To test our first hypothesis, upstream sediment carbon inputs (U_{in}) and sedimentation rates for the two geomorphic zones were estimated via a retrospective erosion assessment, using fallout radionuclide caesium-137 (^{137}Cs) to date floodplain sediments and establish the carbon content of sediment deposited over the last half-century. The degree of protection from decomposition due to burial of sediment-associated carbon, were evaluated using soil aggregate size and density fractionation and the natural abundance δ^{13}C values of the macroaggregates.

2.2.1 | Sedimentation and core chronology

Sediment deposition rates in the 11 floodplain cores were calculated utilizing ^{137}Cs content, determined by gamma spectrometry on 40 g, oven-dried, subsamples of surface sediment and at 2 cm soil core depth increments, sieved to 63 μm prior to analysis using an ORTEC GMX co-axial HPGe γ-detector at 661.67 KeV (AMTEC, TN, USA). Sedimentation rates were subsequently calculated by determining the depth in the profile where the maximum ^{137}Cs peak was identified,
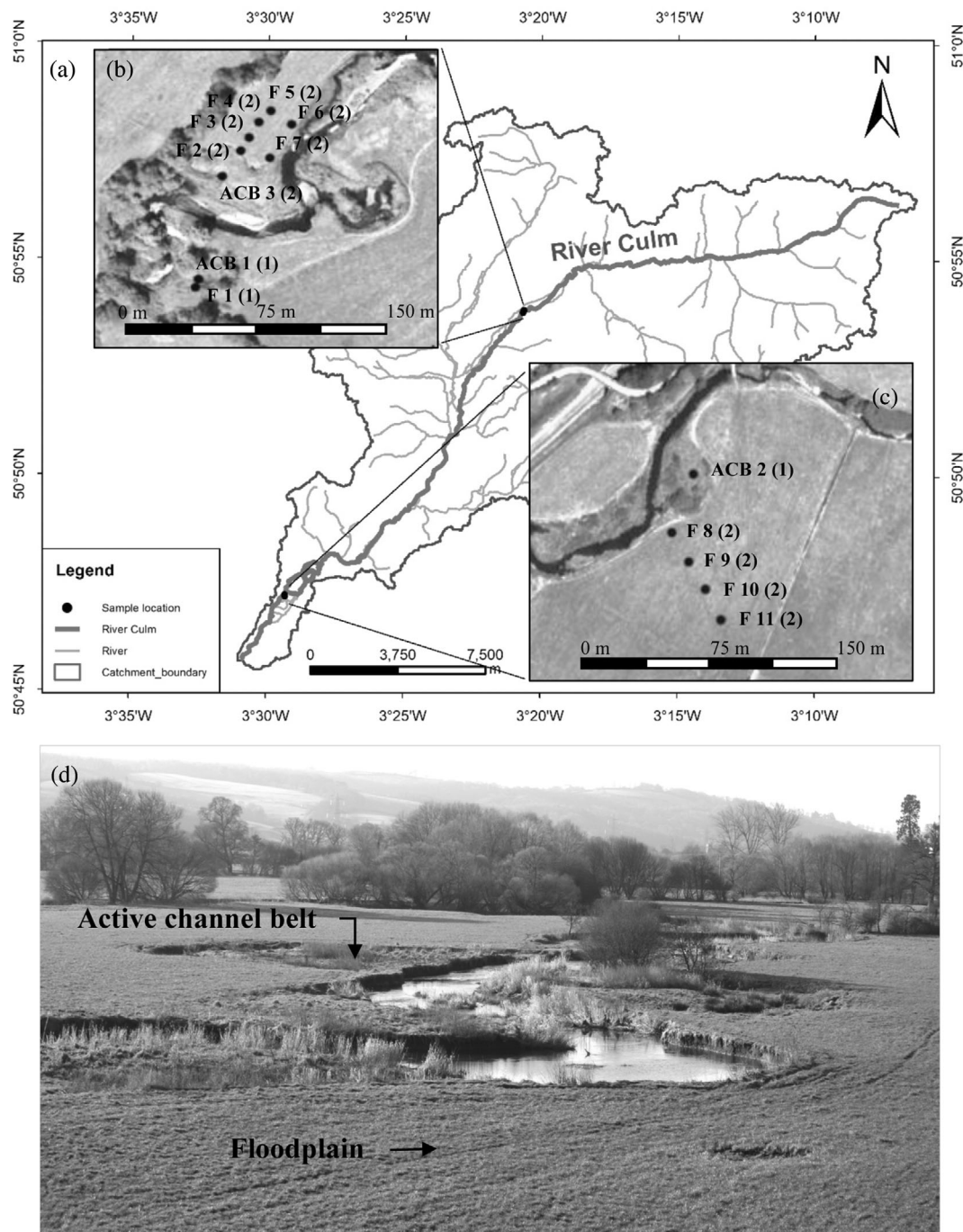
FIGURE 1 Schematic of the (a) river Culm catchment, Devon UK. Lowland grassland sampling locations at (b) Smithincott (50°33′50.2″ N, 3°20′34.8″ W) and (c) Rewe (50°47′15.2″ N, 3°29′20.0″ W); (d) an example of the floodplain at Rewe, with ACB and lowland floodplain (F) indicated. Sampling times April 2008 (1) and October 2008 (2), imagery accessed via Google earth

assumed to occur at 1963 at the peak of atomic bomb testing (Quine & Van Oost, 2007; Yan et al., 2002), using the equation:

$$\text{Activity (mBq/g)} = (\alpha \times 10^5 \times DE)/T \times W_t, \qquad (1)$$

where, α is the area (KeV) of the energy spectrum peak produced by the counts of gamma (γ)-rays, DE is the detector efficiency (mBq Kev^{-1} s), T is the counting time (seconds), and W_t is the sample weight (g). Depending on the sample activity, count times ranged from

80 000 to 425 000 s. Activity at date of sampling was corrected for ^{137}Cs half-life (30.17 y) and the time interval from sampling to analysis (Walling & Quine, 1990). In the three ACB cores, channel migration resulting in channel abandonment and cut-off formation occurred in 1974: ACB-1, 1963: ACB-2, and 1998: ACB-3, enabling the sedimentation rate to be estimated from the depth of sediment above the gravel layer.

The chronology of the ACB and floodplain cores were estimated following the identification of the peak in ^{137}Cs activity attributed to

TABLE 1 Selected properties of the river Culm, the longest tributary of the river Exe, in SW England, UK, data from Hooke (1977), UK National River Flow Archive, Walling et al. (2006)

Property	
Catchment	226 km^2
River length	40 km
Mean altitude	140 m
Maximum altitude	295 m
Mean annual precipitation	952 mm
Mean annual temperature	10.5°C
Catchment slope	11.5 m km^{-1}
Dominant catchment land use:	
Pasture	53.6%
Arable	29.0%
Bank height	1.25 m
Normal flow height range	0.24–1.20 m
Average discharge	3.8 m^3 s^{-1}
Estimated sediment yield	25 t km^{-2} y^{-1}
Average maximum lateral movement	12.5 m
Length of river eroding	17.5 %

1963 (Quine & Van Oost, 2007) or known cut-of formation date. Age is estimated by dividing depth by the calculated sedimentation rate (assuming constant sedimentation rates and no vertical mobilization of the ^{137}Cs in the soil profile).

2.2.2 | Carbon supply with upstream sediment (U_{in}) addition

Geomorphic variation in carbon deposition, associated with sedimentation, was estimated using the relationship of silt and clay with carbon (Torres-Sallan et al., 2017; Supporting Information S.1, S.2, and S.3). U_{in} total carbon content was determined for surface sediment samples ($n = 39$) and the cores ($n = 14$) at 2 cm depth increments from 0.0 to 0.8 m. Samples were oven-dried and sieved to 2 mm prior to analysis on a Flash 2000 organic elemental analyser (Thermo Scientific, CE Instruments Ltd, Wigan, UK). Particle size distribution was measured using a high-definition digital Saturn DigiSizer (Micromeritics, Saturn DigiSizer™ 5200, Norcross, GA, USA). In order to estimate annual U_{in} of carbon, a Monte Carlo analysis was undertaken for each 2 cm core depth increment, utilizing the silt and clay content of the soil profile and the dry bulk density (determined per 2 cm core increment utilizing the volume of the corer and oven-dried weighed soil; S.2). In the lowland floodplain cores, silt and clay content were consistent over depth, the ACB cores were more variable (S.3).

2.2.3 | Carbon storage quantification

Carbon accumulation rates over the past 45 y (from the 1963 ^{137}Cs activity peak) or from cut-off infilling period, and total carbon stock over the 0.8 m soil profile were determined following analysis of the total carbon in 2 cm depth increments.

2.2.4 | Geomorphic variation in carbon decomposition

The impact of geomorphic variation on carbon availability and decomposition was assessed on the three preliminary March 2008 cores (ACB-1, ACB-2, and F-1), via aggregate size and density fractionation, and δ^{13}C analysis. Surface sediment samples ($n = 39$) and 31 samples from the three preliminary March 2008 cores (ACB-1, $n = 6$; ACB-2, $n = 9$; and F-1, $n = 8$; samples from 0 to 0.8 m) were separated via gentle wet sieving into aggregate size fractions >2000, >250, >53, and <53 μm. A subset of oven-dried aggregates from 15 surface sediment samples and all wet sieved core samples were subsequently fractionated into five categories: mineral-associated SOC (mSOC), fine intra-aggregate particulate organic matter (iPOM), coarse iPOM, >2000 μm and light fraction (LF) according to Six et al. (1998), before determination of total carbon on all fractions.

The coarse macroaggregate fraction (>2000 μm) was further separated into five categories by density fractionation: mSOC, fine iPOM, coarse iPOM, >2000 μm and LF, and analysed for δ^{13}C using a SerCon Integra2 isotope ratio mass spectrometer (SerCon Ltd., Crewe, UK) for a subset of core samples (ACB-1, $n = 3$; ACB-2, $n = 4$; F-1, $n = 3$). The δ^{13}C value can be utilized as a proxy for SOC decomposition, as natural abundance ^{13}C-enrichment occurs due to the preferential mineralization of ^{12}C according to the Rayleigh effect of kinetic fractionation (Beniston et al., 2014; Wang et al., 2014). δ^{13}C values were expressed relative to PeeDee Belemnite (PDB; δ^{13}C = -19.58‰ $_{PDB}$) reference material using the equation:

$$\delta^{13}C X‰_{PDB} = \left(\left(R_{sample}/R_{reference} \right) - 1 \right) \times 1000 \qquad (2)$$

where R is the ratio of the heavy isotope over the light isotope and X is the isotope ratio expressed in units of per mille (‰; Glendell et al., 2018).

2.3 | Simulation of residence time of catchment derived floodplain carbon

To test our second and third hypotheses, model simulations were utilized to assess whether carbon MRT varies with geomorphic context, and how carbon storage is affected by the duration of sediment in the ACB. Carbon MRT was evaluated utilizing a simplified model of floodplain carbon storage applied retrospectively to estimate the net carbon exchange between floodplain and atmosphere (Figure 2). Where the difference between inputs of carbon from vegetation (A_{in}) and U_{in} and the atmospheric loss of carbon (A_{out}) enabled the exploration of floodplain storage (ΔFPS) and atmospheric carbon exchange over decadal timeframes. First, A_{out} was determined using RothC decay coefficients enabling the perturbation in decomposition to be estimated depending on geomorphic zone. Second, the scale and
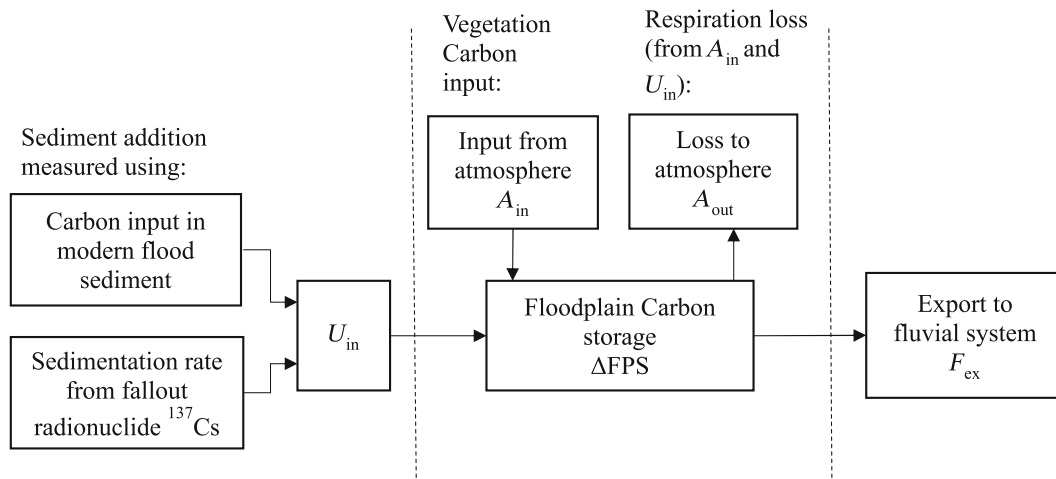
FIGURE 2 Simplified model of floodplain carbon storage, where the floodplain store of SOC is increased by deposition of SOC in association with sediment, derived from upstream catchment soils (U_{in}) and by production of SOC from photosynthate derived from in situ plants (A_{in}). The store is depleted by respiration of SOC and release to the atmosphere (A_{out}) of CO_2 and CH_4 and by channel bank erosion (F_{ex}). Therefore, the change in floodplain carbon storage ΔFPS is defines as follows:

$$\Delta FPS = [U_{in} + A_{in}] - [A_{out} + F_{ex}] \tag{3}$$

In the context of this investigation, the property of greatest interest is the direction and magnitude of net exchange between the floodplain and the atmosphere. At the scale of the entire floodplain, this requires knowledge of all elements in Equation (3); however, at the scale of individual locations on the floodplain, F_{ex} can be excluded by examining locations subject to net accretion and net exchange can be defines as follows:

$$[A_{in} - A_{out}] = \Delta FPS - U_{in} \tag{4}$$

significance of the difference in decomposition between the ACB and floodplain soils was assessed utilizing the mechanistic floodplain evolution model of Schwendel et al. (2015) coupled with RothC decay coefficients and the calculated decomposition perturbation coefficient between the two zones.

First, we evaluated the impact on carbon MRT in the two geomorphic zones using RothC. Estimated U_{in} and A_{in} inputs (Figure 2) were decayed utilizing the established pathways and decay rates of RothC (Supp S.4; Coleman & Jenkinson, 2014). To validate the RothC decay model output, modelled carbon content was compared to the observed data from the 14 cores, enabling the impact of geomorphic variation on carbon MRT to be explored. Carbon MRT was estimated as the sum of the carbon remaining at each iteration by the total added carbon (U_{in} and A_{in}) after 1000 iterations of the RothC decay coefficients. Sediment carbon inputs (U_{in}) were calculated (detailed in *2.2.2*) and were compartmentalized, utilizing the surface sediment samples density separation data ($n = 15$; detailed in *2.2.4*), into the five RothC model pools (decomposable plant material—DPM: 11.2%; resistant plant material—RPM: 7.8%; soil microbial biomass—BIO: 1.2%; humified organic matter—HUM: 71.7%; and inert organic matter—IOM: 8.1%). The proportion of DPM and RPM in U_{in} was calculated from the density-separated LF (assumed to be DPM), and applying the 1.44 DPM:RPM ratio (Coleman & Jenkinson, 2014). BIO was estimated using the average topsoil soil microbial biomass calculated in Cressey et al. (2018) from these sites (1.2 ± 0.1% of total

carbon). IOM was calculated as per Falloon, Smith, Coleman, et al. (1998) from total carbon, and HUM was estimated to be the remainder carbon formed from mSOC, fine and coarse iPOM (Zimmermann et al., 2007). A range of A_{in} values were explored (1.70 t C ha^{-1} y^{-1}: Coleman & Jenkinson, 2014; 2.40 t C ha^{-1} y^{-1}: Batson et al., 2015; 3.70 t C ha^{-1} y^{-1}: Falloon, Smith, Smith, et al., 1998; 5.15 t C ha^{-1} y^{-1}: Meersmans et al., 2013). A_{in} was also divided in to DPM and RPM using the ratio 1.44 (DPM:RPM) in RothC (Coleman & Jenkinson, 2014). However, unlike U_{in} which is added to the surface, A_{in} was added to the decomposition model exponentially as a function of depth.

Secondly, the impact of geomorphic variability in floodplain environments on carbon storage was simulated by combining the floodplain evolution model of Schwendel et al. (2015) with RothC decay coefficients. This floodplain model represents overbank sedimentation as a function of floodplain elevation and distance from the active channel (Moody & Troutman, 2000). River migration is modelled using the approach of Howard and Knutson (1984), modified to include chute cutoffs. Channel migration leads to erosion (removal) of floodplain sediment down to the level of the river bed, and also to the creation of new floodplain surfaces (point bars) where sediment and associated carbon can begin to accumulate. Bend cutoff leads to channel abandonment, which also promotes the creation of new floodplain surfaces in former river locations. The model parameters were defined to generate a channel-floodplain system with

characteristics matching those of the river Culm, using data measured from the river Culm: mean channel sinuosity ~1.5; mean channel migration rate ~0.2 m y^{-1} (Hooke, 1980); mean channel width and depth ~12 m and 1.5 m, respectively; and mean floodplain sedimentation rate ~0.5 mm y^{-1} (Lambert & Walling, 1987). RothC was implemented as described above and defined by the flood deposit samples collected here. Carbon inputs to the floodplain were further partitioned into two pools representing material stored above and below a vertical datum separating the dry (above) and wet (below) portions of the floodplain soil column. Modelled carbon decay rates for the wet and dry floodplain stores were defined following the analysis of the laboratory data using RothC (described below 3.3), which involves perturbation of carbon decomposition rates in the wet parts of the soil profile by a factor of 0.25. The vertical datum used to separate wet and dry sections of the floodplain soil profile was located 1.2 m above the river bed (as observed in the cores). Modelled carbon storage values are a product of geomorphic processes (calibrated to reproduce the characteristics of the river Culm) and carbon decay rates (calibrated using the laboratory data). These carbon storage values were validated independently against samples from the floodplain sediment cores.

2.4 | Statistical analysis

Statistical procedures were undertaken using the software package SPSS v25 for Windows (SPSS Inc., Chicago, IL) and Microsoft Excel, with $p < 0.05$ used as the upper limit for statistical confidence. Comparisons between the empirical data from the ACB and floodplain zones were compared using one-way ANOVA or Kruskal–Wallis where the assumption of equal variance was not met. The measured soil profile carbon data versus estimated carbon supply from the inputs of U_{in} and A_{in} decayed using RothC were also compared using one-way ANOVA. Error is reported for average data with ±standard error of the mean (SEM). Data from Rewe and Smithincott were amalgamated to provide an estimate of carbon dynamics for this lowland section of the river Culm. The dataset supporting this study is available at Quine et al. (2021).

3 | RESULTS

3.1 | Empirical assessment of carbon in the lowland culm floodplain

3.1.1 | Carbon storage

We observed significant differences between the two geomorphic zones across measured soil parameters ($p < 0.05$; Table 2). Carbon concentration declined exponentially in floodplain soils from the topsoil (0–0.2 m) to the deepest section of subsoil (0.7–0.8 m; Table 2). By comparison, ACB cores demonstrated no reduction in subsoil carbon, and three-fold more subsoil carbon was measured in the ACB

compared to the floodplain. Sedimentation rates in the ACB and floodplain cores were significantly different (ACB: 1.93 ± 0.30 cm y^{-1}; floodplain: 0.35 ± 0.03 cm y^{-1}; $p < 0.05$; S.2). Carbon accumulation rates also varied significantly between the geomorphic zones (ACB: 5.18 ± 1.19 Mg C ha^{-1} y^{-1} over 25 y and 4.67 ± 0.29 Mg C ha^{-1} y^{-1} over 50 y—only two cores exceeded 25 y in the ACB decreasing variation; floodplain cores: 0.93 ± 0.07 Mg C ha^{-1} y^{-1} over 25 y and 0.91 ± 0.08 Mg C ha^{-1} y^{-1} over 50 y; $p < 0.05$; S.5; core chronology was estimated from the sedimentation rates to enable comparisons between geomorphic zones).

Surface sediment samples had a two-phase relationship between carbon and silt and clay content, with a division between large and small carbon content (S.1). Of the measured sediment properties, only ^{137}Cs content and wet sieved aggregate size separation correlated to the two-phase carbon content in the surface sediment. Sediment with both small and large carbon contents is likely to have originated from within the catchment; with low carbon content samples probably originating from channel bank erosion and high carbon content from topsoil (Walling, 2005; Table 2; S.1). A significantly greater proportion of wet sieved macroaggregates (>2000) was present in the large carbon content group (large carbon content: 53.2 ± 6.1% macroaggregates mass, small carbon content: 7.1 ± 2.5% macroaggregates mass), with a linear correlation observed between the percentage mass of >2000 μm aggregates and the total carbon measured in the sediment samples ($r^2 = 0.79$; Figure 3; $p < 0.05$). Although a weaker correlation, a similar trend was observed in the core samples, with total carbon increasing with the proportion of aggregates present in the >2000 μm fraction ($r^2 = 0.34$; Figure 3). ACB soils were dominated by macroaggregates, with 71.6 ± 4.3% mass present in the >2000 μm fraction compared to 27.6 ± 4.0% >2000 μm mass in the floodplain cores.

3.1.2 | Carbon processing

Physical protection of carbon also varied with geomorphic zone (Figure 3). A greater proportion of carbon was allocated to mSOC in the floodplain compared to ACB and surface sediment samples (surface sediment: 26.7 ± 2.0% C, ACB: 37.9 ± 5.1% C, floodplain: 72.0 ± 5.0% C; Figure 3). There was no significant difference in the percentage of mSOC between 0 and 20 y and 20–50 y in the ACB soil (0–20 y: 40.0 ± 5.4% C; > 20 y: 34.8 ± 10.3% C), whereas in the floodplain cores, a greater proportion of mSOC was found in soil >20 y (0–20 y: 57.6 ± 11.8% C; > 20 y: 76.8 ± 4.4% C). Carbon preservation in the ACB > 20 y soil was distributed across all fraction sizes, including the LF. However, in the floodplain soil, there was no preservation of the LF in the >20 y soil, and <13% in each of the fine iPOM, coarse iPOM and gravel fractions, compared to 19.3 ± 8.4% LF and >14% in POM fractions in the >20 y ACB soil. Surface sediment carbon was distributed across all fractions (Figure 3).

Alongside the dominance of mSOC in the floodplain soil, there were more enriched δ^{13}C values in the >20 y floodplain macroaggregate fraction (>2000 μm; ACB: −28.5 ± 0.1‰, floodplain: −26.6 ± 0.2‰; Figure 4; raw data S.6). However, there was no difference in

TABLE 2 Selected soil and surface sediment properties, with soil samples averaged over 10 cm depth increments

Soil properties					
Sample depth (cm)	Silt (%)	Clay (%)	Moisture content (%)	Total Carbon (g kg^{-1})	Cumulative Cs (Bq kg^{-1})
Active channel belt					
0–10	66.51 ± 2.78	12.03 ± 0.88	50.35 ± 4.06	70.30 ± 7.93	111.57 ± 28.56
10–20	63.28 ± 3.39	12.04 ± 0.87	33.54 ± 1.84	42.67 ± 4.32	101.16 ± 22.15
20–30	71.07 ± 2.43	14.42 ± 1.01	38.72 ± 2.16	50.12 ± 3.54	114.32 ± 21.61
30–40	73.37 ± 1.07	15.10 ± 0.85	42.95 ± 1.80	56.48 ± 4.78	109.39 ± 7.92
40–50	71.06 ± 1.53	14.64 ± 0.85	47.18 ± 1.65	61.13 ± 4.67	80.83 ± 10.44
50–60	68.55 ± 1.97	13.43 ± 0.77	46.69 ± 1.99	57.77 ± 3.58	61.27 ± 8.15
60–70	63.36 ± 3.66	12.86 ± 0.72	45.79 ± 3.40	49.25 ± 6.80	36.70 ± 5.43
70–80	58.35 ± 3.01	12.77 ± 1.00	47.97 ± 3.78	42.24 ± 7.12	26.34 ± 3.78
Floodplain					
0–10	68.71 ± 1.01	16.61 ± 0.65	36.98 ± 1.51	53.27 ± 3.57	100.46 ± 6.64
10–20	70.16 ± 0.76	17.63 ± 0.46	31.49 ± 0.72	39.16 ± 2.41	58.48 ± 4.46
20–30	68.96 ± 0.68	16.75 ± 0.49	27.92 ± 0.76	27.57 ± 2.20	13.22 ± 2.46
30–40	68.46 ± 0.82	16.03 ± 0.42	23.03 ± 0.27	14.79 ± 0.70	1.81 ± 0.51
40–50	73.73 ± 0.76	16.95 ± 0.31	23.53 ± 0.36	14.80 ± 0.50	0.37 ± 0.27
50–60	76.64 ± 0.92	18.51 ± 0.67	24.85 ± 0.27	15.00 ± 0.59	0.97 ± 0.58
60–70	74.53 ± 1.05	19.75 ± 0.89	23.45 ± 0.58	13.91 ± 0.52	0.00
70–80	63.85 ± 1.90	24.49 ± 1.32	21.50 ± 0.31	8.08 ± 0.86	0.00
Geomorphic	*	*	*	*	*
Depth	*	NS	*	*	*
Surface sediment					
Low Cs-137	46.81 ± 2.28	9.78 ± 0.53	14.53 ± 1.84	8.13 ± 0.88	0.80 ± 0.12
High Cs-137	58.20 ± 1.81	10.68 ± 0.46	45.09 ± 2.93	38.33 ± 4.20	3.50 ± 0.27
Surface sediment	*	NS	*	*	*

Note: Values represent means ± SEM ($n > 6$). The symbols * indicate the significant differences at the $p < 0.05$ level between geomorphic areas on the lowland river Culm floodplain and over depth, with NS denoting samples with no significant differences. Significant differences between high and low Caesium-137 groups of surface sediment is also given (* for significant differences at the $p < 0.05$ level and NS denoting non-significant differences).
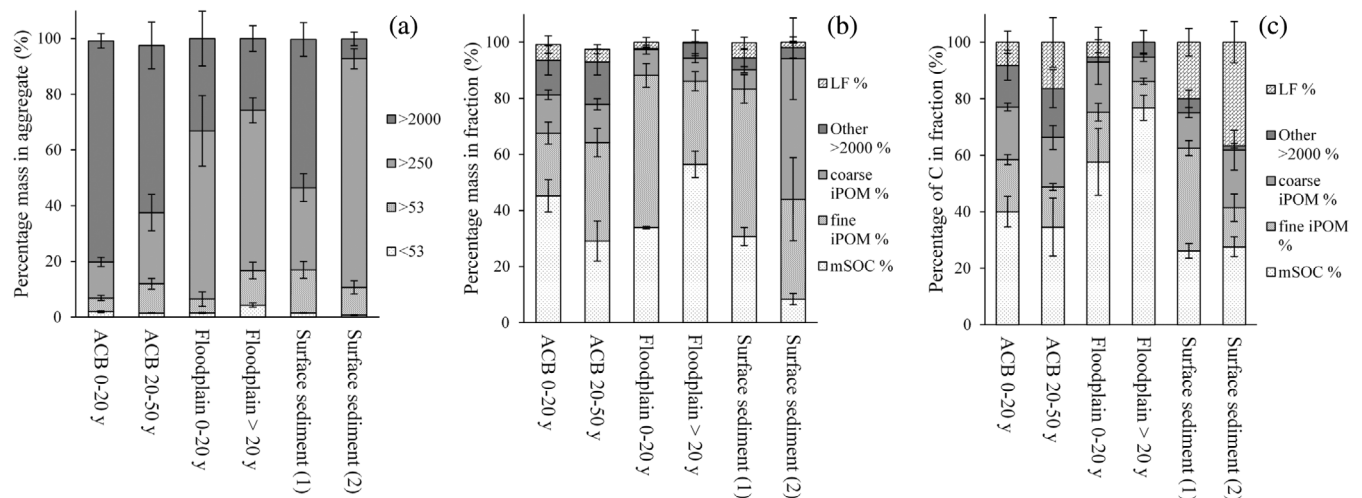
FIGURE 3 Fractionation by geomorphic location between the surface sediment samples the ACB and the floodplain. Where the age profile is estimated from the ^{137}Cs assay: ACB 0–20 y ($n = 9$) 20–50 y ($n = 6$) from cores ACB-1 ACB-2; floodplain 0–20 y ($n = 2$) and >20 y ($n = 6$) core F-1. Error is SEM for the surface sediment ($n = 15$) ACB and floodplain cores. (a) The mass distribution from gentle aggregate separation (%). (b) The mass distribution following density separation into mSOC fine iPOM coarse iPOM macroaggregates >2000 μm and LF (%). (c) The proportion of carbon within each fraction following density separation (%)
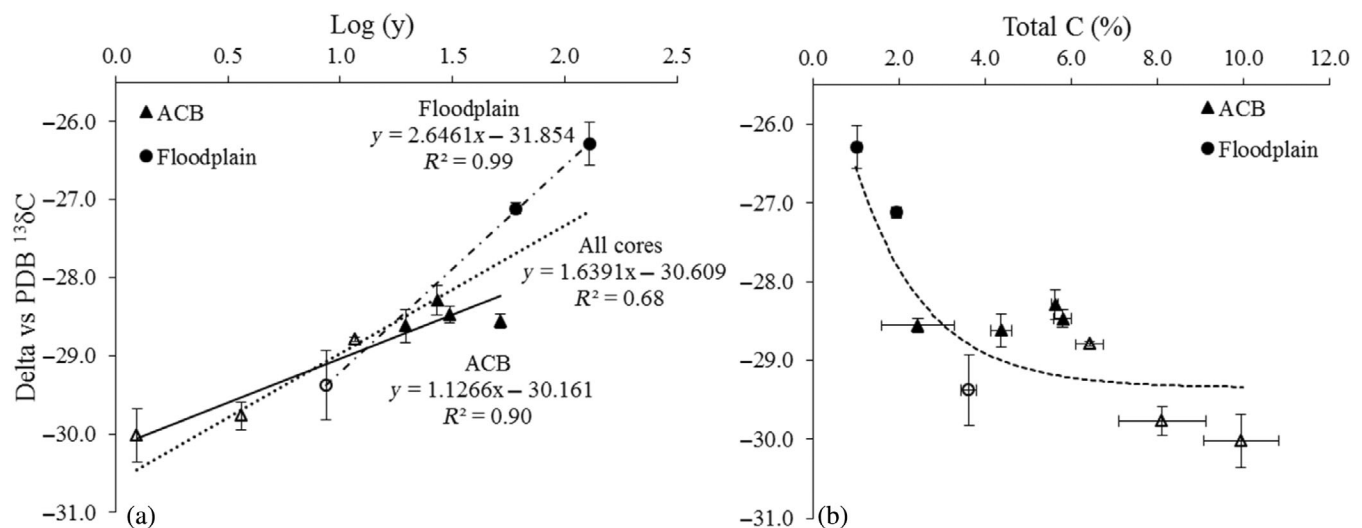
FIGURE 4 $\delta^{13}C$ values of the macroaggregate >2000 μm density separated fraction for selected samples from the ACB and floodplain (ACB: $n = 7$ and floodplain: $n = 3$; cores ACB-1, ACB-2, and F-1). (a) The linear relationship of $\delta^{13}C$ versus log(age) is shown for all samples and separated for the high and low deposition samples. Age is estimated from the ^{137}Cs assay, empty symbols are <20 y. Error is SEM for the fractions (mSOC, fine iPOM, coarse iPOM, >2000 μm and LF analysed at each depth). (b) Comparison of $\delta^{13}C$ to total carbon (%), the exponential decline in $\delta^{13}C$ with increasing carbon (%) is shown

<20 y soils between geomorphic zones (ACB: $-29.5 \pm 0.2‰$, floodplain: $-29.4 \pm 0.4‰$). Two linear relationships could be observed, with the ACB demonstrating a less rapid increase in $\delta^{13}C$ values over time suggesting reduced microbial processing had occurred (Figure 4). Similarly, $\delta^{13}C$ values increased exponentially with decreasing carbon content (Figure 4; $R^2 = 0.67$). However, these relationships are based on a small sample number and would benefit from further investigation.

## 3.2 | Simulation of catchment derived carbon

3.2.1 | RothC carbon dynamics

Carbon inputs from sediment—U_{in} and vegetation—A_{in} were decayed using RothC decay coefficients and compared to the empirical data (Figure 5). A range of vegetation inputs from 0.17 to 0.52 kg C m^{-2} y^{-1} were investigated, however, varying vegetation inputs did not significantly impact modelled outputs; only applying a sediment only addition, that is, with no vegetation, resulted in a significant change (S.5). In floodplain cores, RothC decay of U_{in} and A_{in} resulted in a close 1:1 fit to observed core profile data ($r^2 = 0.90$; Figure 5; S.7). In the ACB, RothC decay coefficients underestimated the amount of carbon retained within the soil profile and a weaker linear regression was observed ($R^2 = 0.68$; Figure 5; S.7). Reducing the rate of decomposition by a factor of 0.25 resulted in a reduction in the underestimation between modelled and observed carbon contents, with an improved linear regression ($R^2 = 0.90$; Figure 5; S.7).

The 0.25 rate perturbation applied to the ACB cores reduced the simulated loss of carbon as A_{out} from $75 \pm 2\%$ to $55 \pm 3\%$ after 50 y, which was comparable to the approximate $52 \pm 11\%$ loss of carbon

observed in the ACB cores by 0.8 m (as compared to topsoil carbon content; Figure 5; S.5).The RothC model overestimated carbon loss (A_{out}) in the floodplain cores, where by 150 y (estimated age at 0.8 m) $94 \pm 1\%$ of the added carbon had been lost, whereas approximately $73 \pm 4\%$ loss was observed by 0.8 m (compared to topsoil carbon; Figure 5; S.5). In the floodplain cores, the decline in carbon content over depth stabilized after 0.4 m, suggesting decomposition rate perturbation below 0.4 m depth (Table 2), which was used as the threshold depth for wetness in the binary wet/dry model below. Carbon MRT increased linearly with increasing deposition rate ($R^2 = 0.63$: no rate perturbation applied; $R^2 = 0.84$: with ACB 0.25 rate perturbation). In low deposition floodplain soils carbon MRT averaged 43 ± 3 y, rate perturbation in the ACB increased carbon MRT to 157 ± 14 y (S.5). Reducing vegetation inputs (A_{in}) increased MRT as the impact of rapid cycling A_{in} was reduced and the dominance of slower cycling carbon pools in U_{in} was more pronounced (U_{in} only model—floodplain carbon MRT: 125 y, ACB with rate perturbation: 252 y; S.5).

3.2.2 | Catchment carbon dynamics

The binary floodplain evolution model, coupled with the RothC parameters above, was utilized to evaluate the effect of geomorphic processes on carbon sequestration potential, with the net exchange of carbon to the atmosphere determined by the length of time sediment resides in the ACB and carbon MRT. An elevation of 1.2 m above the channel was utilized as the wetness boundary between slow and rapid decomposition rates. The area of ACB had the greatest implication for carbon storage within the floodplain (Figure 6), total carbon storage reduced as sedimentation increased, due to increasing floodplain elevation resulting in drier conditions fostering more rapid
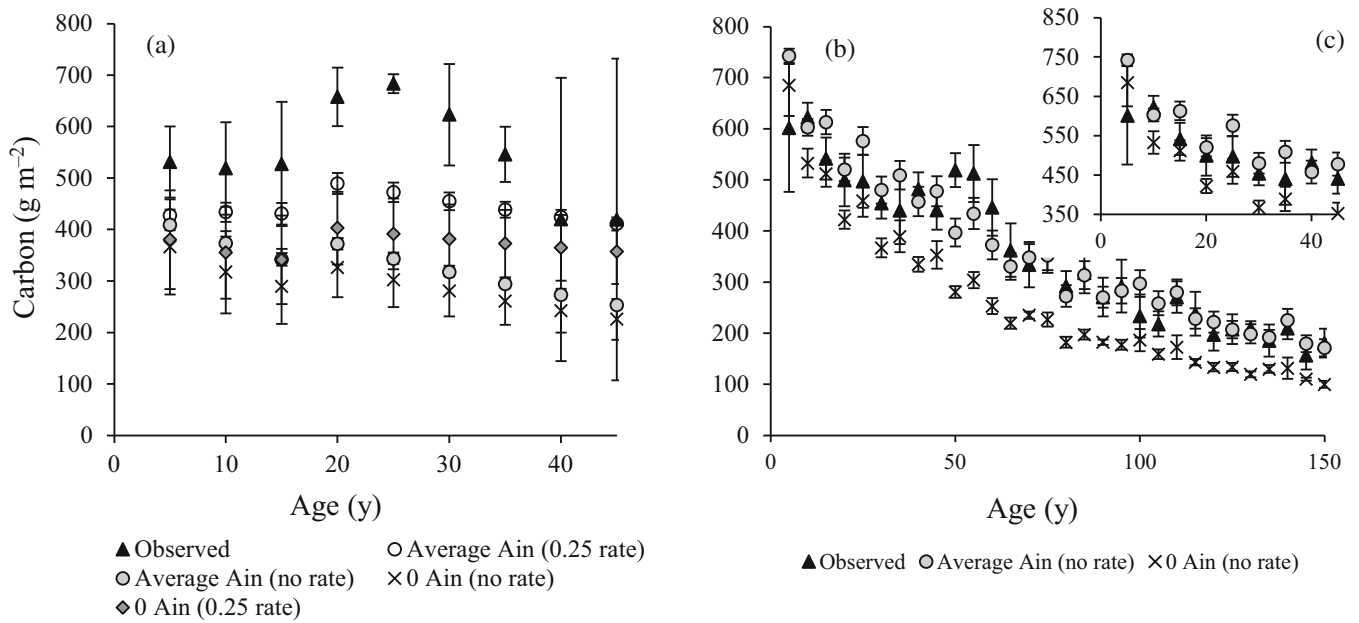
FIGURE 5 Measured carbon content averaged across 5 y intervals for the ACBs (a; $n = 3$) and floodplain (b; $n = 11$) cores on the river culm, with the age profile estimated from the ^{137}Cs assay or from cut-off formation. ACB cores reached the bedload at approx. 45 y compared to >150 y for floodplain cores. With panels (a) and (b) showing the observed carbon to the modelled carbon and the inset panel (c) the floodplain carbon content over 45 y. Modelled carbon utilized RothC decay coefficients applied to estimates of U_{in} and A_{in}, with average vegetation input of 3.24 t C ha^{-1} y^{-1} and sediment only (0 A_{in}) model outputs shown. Panel (a) shows the modelled carbon in ACB cores using RothC decay coefficients with the rate adjustment factor (0.25 rate) and without rate adjustment (no rate)
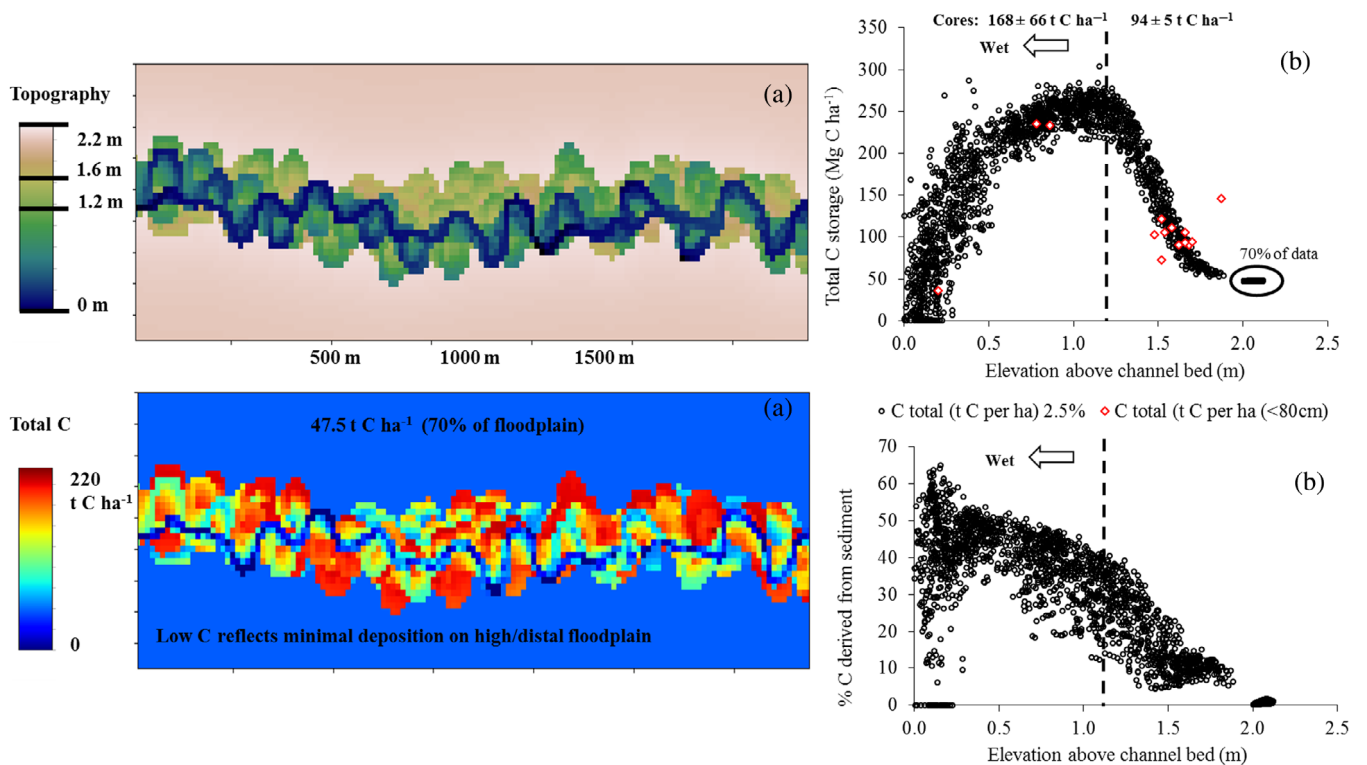
FIGURE 6 Floodplain evolution model demonstrating lowland floodplain topography and associated carbon storage (a); modelled carbon storage and % carbon derived from U_{in} (b), utilizing the elevation of 1.2 m above the channel bed as the boundary between RothC decay rates and the rate perturbed 4-fold slower decomposition in the high deposition ACB, with observed field data of carbon stock over 0.8 m (ACB: $n = 3$, floodplain: $n = 11$; panel b).

decomposition rates. The most active floodplain portions of the lower elevation ACB, where sedimentation and reworking rates were greatest, stored more carbon than the inactive floodplains due to the high rates of carbon delivery and estimated four times slower decomposition, and also due to the shorter sediment residence times due to reworking (i.e., giving carbon less time to decompose).

The floodplain evolution model estimated the total floodplain carbon in the ACB area to be 173 ± 2 t C ha^{-1}, which is comparable to the measured empirical data of 168 ± 66 t C ha^{-1}. Modelled carbon content for the floodplain area underestimated stored carbon (observed: 94 ± 5 t C ha^{-1}; modelled: 60 ± 1 t C ha^{-1}; Figure 6), however, the sampled floodplain cores were adjacent to the channel, less than 2 m elevation, and it is likely this contributes to the underestimation. The model indicates a large area of distal floodplain receiving minimal sediment inputs, but having rapid decomposition (average modelled carbon content in distal floodplain >2.0 m elevation $48 \pm <0.01$ t C ha^{-1}, forming approximately 70% of the floodplain). There is large variation in the carbon content of the ACB, with modelled values ranging from 0 to 304 t C ha^{-1}, due to areas of recent channel migration having very low elevation and less carbon content, which is also observed in the large variation in the measured ACB cores. Based on digitization of the Culm catchment, the estimated area of ACB was 0.02 km^2 and the lowland floodplain near the channel 1.88 km^2, the calculated overall MRT of carbon increased by approximately 10% from 43 y in the floodplain soils to 48 y when the slower, rate perturbed ACB areas were accounted for (157 y carbon MRT in the ACB cores).

4 | DISCUSSION

4.1 | Empirical assessment of carbon storage in the lowland culm floodplain

In this paper, we tested the hypothesis that carbon storage varies with geomorphic context. We found, as in Mayer et al. (2018), significant variation in subsoil carbon stocks between geomorphic zones. Floodplain soils exhibited an exponential decrease in carbon with increasing depth, potentially due to the dependence on autochthonous (vegetation) carbon additions in these mineral soils and suggestive of limited hydrological connectivity increasing mineralization rates (Hinshaw & Wohl, 2021; Lininger et al., 2018; Ricker et al., 2012). In contrast, carbon in the ACB did not decrease significantly with depth, this diverse vertical structure has been observed in other saturated wetlands, marshes, peatlands and soils in depositional areas (D'Elia et al., 2017; Mayer et al., 2018). Carbon accumulated at significantly greater rates in the ACB than the floodplain (4.7 ± 0.3 Mg C ha^{-1} y^{-1} compared to 0.9 ± 0.1 Mg C ha^{-1}), though within the riparian soil range reported in Hinshaw & Wohl (2021; 0.03–12.2 Mg C ha^{-1} y^{-1}). Topsoil (0–0.2 m) carbon stock was unaffected by landform position (averaging 51 ± 2 Mg C ha^{-1}), suggesting the rapid turnover of recent plant inputs controlled topsoil carbon dynamics (Mayer et al., 2018; Scheingross et al., 2021; Wang et al., 2014). Whereas, there was significant

geomorphic variation when subsoils were included (to a depth of 0.8 m or to the bedload; 98 ± 6 Mg C ha^{-1} in the floodplain and 168 ± 66 Mg C ha^{-1} in the ACB). Therefore, it is important to consider the whole profile when assessing carbon storage.

The significantly greater sedimentation rates in the ACB highlights the need to include different topographical zones in riparian studies (ACB: 19 ± 3 mm y^{-1}, floodplain: 3.5 ± 0.3 mm y^{-1}; Mayer et al., 2018; Scheingross et al., 2021; Wohl et al., 2017). The sedimentation rates in these heavily altered systems were similar to the post-colonial rates in southern New England (0.3–10 mm y^{-1}; Ricker et al., 2012). Sediment carbon (U_{in}) was also highly variable (0.2–8.1% C), potentially due to bank erosion mobilizing older organic matter or from the preferential transport of LF during flood events contributing to the range of carbon deposition values (Lal, 2019; Lininger et al., 2018; Walling, 2005; Wohl et al., 2017). The average U_{in} of 2.1 ± 0.3% carbon was within the range reported in similar UK rivers (2–5%; Walling et al., 2006). The allochthonous U_{in} carbon was significantly lower than topsoil carbon, which indicates the potential for these systems to sequester carbon from in situ autochthonous vegetative production on bare sediment surfaces (Graf-Rosenfellner et al., 2016; Lininger et al., 2018; Ricker et al., 2012).

We evaluated our second hypothesis, that decomposition varies with geomorphic zone, utilizing soil aggregate size, density fractionation and stable ^{13}C isotope analysis. Long-term preservation of SOC stocks may rely upon soil stabilization processes from progressive microbial transformation to more stable forms, and not only through new input of carbons, that is, as LF and macroaggregate SOC become physically protected as mSOC or within microaggregates (D'Elia et al., 2017; Graf-Rosenfellner et al., 2016; Lal, 2019; Sutfin et al., 2016; Torres-Sallan et al., 2017; Wang et al., 2014; Wiesmeier et al., 2019). This was observed in the floodplain subsoil, where the proportion of mSOC increased over depth alongside increasingly enriched δ^{13}C values, and there was no evidence of LF preservation. In contrast, ACB carbon was preserved in all aggregate and density fractions, including the free LF over the profile (0–0.8 m). Hydrologic connectivity can regulate carbon decomposition (Sutfin et al., 2021), suggesting preservation in the ACB was due to the soil conditions, that is, persistent water saturation reducing microbial processes, rather than the inherent carbon recalcitrance (ACB moisture content: 44 ± 2%, floodplain: 27 ± 2%; Mayer et al., 2018; Scheingross et al., 2021). Irrespective of geomorphic location, mSOC and microaggregates were the dominant fractions; indicating the potential for longer-term SOC storage in this stable fraction (Graf-Rosenfellner et al., 2016; Van Oost et al., 2012; Wiesmeier et al., 2019).

4.2 | Simulated floodplain carbon dynamics

Having measured variable geomorphic carbon storage, residence time of carbon within these landform positions must be evaluated to assess whether sedimentation can act as a sequestration mechanism (Rosenbloom et al., 2006; Sutfin et al., 2016). We utilized two modelling approaches to simulate residence time, first, geomorphic zone

MRT was estimated through RothC decay of carbon inputs. Carbon MRT in the floodplain soils (43 y), although similar to the calculated global average SOC MRT (32 y; Raich & Schlesinger, 1992), was shorter than temperate grassland (61 y; Raich & Schlesinger, 1992) and similar mineral soils with >50% of SOC mineral-bound (topsoil MRT: 320 y, subsurface MRT 2560 y; Fontaine et al., 2007). Which supports the findings of Sutfin et al. (2021) and Wohl et al. (2021), where dry, hydrologically disconnected floodplains were found to have rapid decomposition of carbon. The link between hydrological connectivity and decomposition was further evidenced in the floodplain cores where RothC over-estimated net carbon loss (A_{out}) and, in the empirical data, decreasing carbon stocks stabilized at 0.4 m, suggestive of a persistent water table height reducing decomposition and promoting carbon storage. In the ACB, modelled carbon MRT required a rate reduction of 0.25 (significantly increasing MRT: 157 ± 14 y), which was also reflected in the empirical data, where three-fold more carbon was retained in the subsoil, alongside the preservation of LF and macroaggregates, and less $\delta^{13}C$ enrichment compared to floodplain soils. The rate perturbation suggests carbon buried in highly depositional areas may be stable on decadal timescales and accumulation of SOC is possible (Sutfin et al., 2016; Van Oost et al., 2012; Wang et al., 2014). Modelled longer term carbon storage depended on U_{in} rather than A_{in}, as demonstrated by the linear increase in MRT with increasing deposition rates, with plant contributions dominating rapid cycling pools (Omengo et al., 2016; Scheingross et al., 2021).

The small-scale geomorphic variation in carbon deposition in the ACB, a zone <0.01% of the catchment, resulted in an approximate 10% increase in carbon MRT for the lowland floodplain area (floodplain and ACB soils combined). Therefore, geomorphic variation can have a proportionally large impact on floodplain MRT. Our second modelling approach combined a floodplain evolution model coupled with a binary (wet/dry) RothC decay model (dry: RothC decay rate; wet: decay rate reduced by 0.25). According to the model, the floodplain system is not at equilibrium and is still aggrading, with both the ACB and the lowland core areas still accumulating sediment and carbon in excess of the distal floodplain. Downstream sediment aggradation increased the height of the floodplain, reducing hydrological connectivity, and increasing the decomposition rate in our model, thereby reducing the total amount of stored carbon (Lauer & Parker, 2008; Ricker et al., 2012; Sutfin et al., 2021; Wohl et al., 2021). This is likely to be consistent with the current state of many European lowland rivers still responding to anthropogenic disturbance since the Mesolithic period (Brooks & Brierley, 2002; Brown et al., 2018; Lewin & Macklin, 2010).

4.3 | Implications and limitations

Overall, the evidence from the mechanistic exploration of carbon accumulation and decomposition suggests these lowland temperate floodplains represent a small carbon sink over decadal timescales. The carbon fluxes are controlled through a complex balance of decomposition, SOC stabilization, deposition rates, erosion, and channel migration (Ni et al., 2012; Wohl et al., 2017). The Culm system is broadly representative of many heavily managed European rivers, with overbank sedimentation changing complex river systems to single incised meandering channels in mineral alluvial floodplains since the Mesolithic period (Brown et al., 2018). To illustrate the potential magnitude of carbon stored in UK floodplains, we scaled the carbon stock in the floodplain of our Culm study region to the extent of UK (0.01% high deposition: 54 km^2 and 0.1% low deposition: 5364 km^2; data from the UK National River Flow Archive). This scaling suggests a potential stock on the order of 0.9 Tg C in areas with increased rates of deposition and 50.4 Tg C in areas with decreased rates of deposition, assuming the relative extent of these contrasting deposition zones of the Culm is broadly representative of UK floodplains.

Large investments are being made into the re-naturalization of riparian zones in Europe and on the river Culm, which is currently failing water quality standards due to its high sediment load (Brown et al., 2018; Johnson, 2018). Re-naturalization of river corridors has the potential to enhance sequestration by increasing the complexity of both vegetation and river channel, changing from a single channel to an anabranching system with increased areas of hydrological connectivity, increasing bank strength, reducing sediment load through increased deposition, and reduction in channel migration (Brooks & Brierley, 2002; Brown et al., 2018; Wohl et al., 2021). As seen in the wetter ACB cores, re-naturalization could be a useful tool for climate mitigation through enhanced wetland carbon sequestration (Sutfin et al., 2021; Taillardat et al., 2020). Increasing river complexity can create a hotspot for decomposition through water fluctuation in complex areas increasing decomposition of physically protected carbon in dry periods (Berhe & Kleber, 2013; D'Elia et al., 2017; Mayer et al., 2018; Sutfin et al., 2021; Torres-Sallan et al., 2017; Van Oost et al., 2012). In catchments where the proportion of permanent wetland zones are greater the potential to increase carbon storage, through reduced mineralization rates, may be greater, that is, in floodplains containing beaver meadows, riverine carr, fens, swamps salt marsh, mangrove, seagrass and perennial floodplain lakes (Brown et al., 2018; D'Elia et al., 2017; Hupp et al., 2019; Wohl et al., 2021). While these types of wetlands can have significant emissions of CO_2 and methane, the large carbon stocks in these systems suggests naturally functioning wetlands will act as a sink of carbon (Batson et al., 2015; Brown et al., 2018; Gatland et al., 2014; Hinshaw & Wohl, 2021; Isidorova et al., 2019).

Due to the small proportion of the Culm catchment consisting of high deposition areas, the impact on overall loss of carbon from the catchment is small. However, this dual approach of empirical data and modelling provides a framework to investigate carbon storage in other floodplain systems with varying degrees of hydrological complexity. Future studies utilizing this approach would be beneficial to explore the impact of re-naturalization investigating the impact of successional vegetation, changes in hydrology, sediment residence times, and how this will impact on carbon stores and fluxes.

5 | CONCLUSIONS

The results of the empirical and numerical work presented here provide insights into the control on preservation potential exercised by geomorphic context in temperate floodplains, and provide a framework for more extensive exploration of this missing link in the erosion-carbon budget in other systems where increased areas of reduced decomposition are present. The ACB zone had significantly greater carbon accumulation and sedimentation rates than the lowland floodplain. RothC modelled decomposition rates in the ACB were estimated to be four-fold less than in floodplain soils. Including the ACB in floodplain carbon MRT calculations increased the MRT by 10%, highlighting the importance of geomorphic variation. Overall, these temperate grassland floodplains represent a small carbon sink over a decadal timeframe. However, there is a complex balance of inputs versus decomposition rates, with substantial rates of carbon accumulation and larger rates of deposition in predominantly wet areas with slower decomposition rates, and comparatively increased carbon losses in the drier elevated floodplain due to faster decomposition rates. In summary, the magnitude of the carbon flux from the whole floodplain depends to a large extent on the relative magnitude of sediment storage in "active" and "inactive" areas of the floodplain, and there is the potential for re-naturalization projects to increase active areas, potentially increasing the amount of carbon stored in the floodplain.

AUTHOR CONTRIBUTIONS

Timothy A. Quine: Conceptualization, funding acquisition, field sampling, methodology, data analysis, writing-reviewing and editing. **Andrew P. Nicholas**: Funding acquisition, field sampling, methodology, data analysis, writing-reviewing and editing. **Elizabeth L. Cressey**: Field sampling, laboratory investigation, data analysis, writing-original draft, reviewing and editing. **Sarah De Baets**: Investigation, data analysis, writing-reviewing and editing. **Jeroen Meersmans**: investigation, data analysis, writing-reviewing and editing. **Matthew W. Jones**: Investigation, writing-reviewing and editing. **Jennifer A. J. Dungait**: Resources, writing-reviewing and editing.

CONFLICT OF INTEREST

The authors declare no competing interests with respect to the research, authorship and/or publication of this article.

ORCID

Elizabeth L. Cressey https://orcid.org/0000-0002-2535-6420

REFERENCES

Aufdenkampe, A. K., Mayorga, E., Raymond, P. A., Melack, J. M., Doney, S. C., Alin, S. R., Aalto, R. E., & Yoo, K. (2011). Riverine coupling of biogeochemical cycles between land, oceans, and atmosphere. *Frontiers in Ecology and the Environment*, 9(1), 53–60. https://doi.org/10.1890/100014

Batson, J., Noe, G. B., Hupp, C. R., Krauss, K. W., Rybicki, N. B., & Schenk, E. R. (2015). Soil greenhouse gas emissions and carbon budgeting in a short-hydroperiod floodplain wetland. *Journal of Geophysical Research: Biogeosciences*, 120(1), 77–95. https://doi.org/10.1002/2014JG002817

Beniston, J. W., DuPont, S. T., Glover, J. D., Lal, R., & Dungait, J. A. (2014). Soil organic carbon dynamics 75 years after land-use change in perennial grassland and annual wheat agricultural systems. *Biogeochemistry*, 120(1), 37–49. https://doi.org/10.1007/s10533-014-9980-3

Bennett, J. A., Brown, A. G., Schwenninger, J. L., & Rhodes, E. J. (2011). Holocene channel changes and geoarchaeology of the Exe River, Devon, UK, and the floodplain paradox. Geoarchaeology, climate change and sustainability. *Geological Society of America Special Publication*, 476, 135–152. https://doi.org/10.1130/2011.2476(11)

Berhe, A. A., & Kleber, M. (2013). Erosion, deposition, and the persistence of soil organic matter: Mechanistic considerations and problems with terminology. *Earth Surface Processes and Landforms*, 38(8), 908–912. https://doi.org/10.1002/esp.3408

Brooks, A. P., & Brierley, G. J. (2002). Mediated equilibrium: The influence of riparian vegetation and wood on the long-term evolution and behaviour of a near-pristine river. *Earth Surface Processes and Landforms: The Journal of the British Geomorphological Research Group*, 27(4), 343–367. https://doi.org/10.1002/esp.332

Brown, A. G., Lespez, L., Sear, D. A., Macaire, J.-J., Houben, P., Klimek, K., Brazier, R. E., Van Oost, K., & Pears, B. (2018). Natural vs anthropogenic streams in Europe: History, ecology and implications for restoration, river-rewilding and riverine ecosystem services. *Earth-Science Reviews*, 180, 185–205. https://doi.org/10.1016/j.earscirev.2018.02.001

Chaopricha, N. T., & Marín-Spiotta, E. (2014). Soil burial contributes to deep soil organic carbon storage. *Soil Biology and Biochemistry*, 69, 251–264. https://doi.org/10.1016/j.soilbio.2013.11.011

Coleman, K., & Jenkinson, D. S. (2014). *RothC—A model for the turnover of carbon in soil. Model description and users guide*. Rothamsted Research. https://www.rothamsted.ac.uk/sites/default/files/RothC_guide_DOS.pdf

Constantine, J. A., & Dunne, T. (2008). Meander cutoff and the controls on the production of oxbow lakes. *Geology*, 36(1), 23–26. https://doi.org/10.1130/G24130A.1

Cressey, E., Dungait, J., Jones, D., Nicholas, A., & Quine, T. (2018). Soil microbial populations in deep floodplain soils are adapted to infrequent but regular carbon substrate addition. *Soil Biology and Biochemistry*, 122, 60–70. https://doi.org/10.1016/j.soilbio.2018.04.001

D'Elia, A. H., Liles, G. C., Viers, J. H., & Smart, D. R. (2017). Deep carbon storage potential of buried floodplain soils. *Scientific Reports*, 7(1), 1–7. https://doi.org/10.1038/s41598-017-06494-4

Doetterl, S., Stevens, A., Van Oost, K., Quine, T. A., & Van Wesemael, B. (2013). Spatially-explicit regional-scale prediction of soil organic carbon stocks in cropland using environmental variables and mixed model approaches. *Geoderma*, 204, 31–42. https://doi.org/10.1016/j.geoderma.2013.04.007

Falloon, P., Smith, P., Coleman, K., & Marshall, S. (1998). Estimating the size of the inert organic matter pool from total soil organic carbon content for use in the Rothamsted carbon model. *Soil Biology & Biochemistry*, 30(8–9), 1207–1211. https://doi.org/10.1016/S0038-0717(97)00256-3

Falloon, P., Smith, P., Smith, J. U., Szabo, J., Coleman, K., & Marshall, S. (1998). Regional estimates of carbon sequestration potential: Linking the Rothamsted carbon model to GIS databases. *Biology and Fertility of soils*, 27(3), 236–241. https://doi.org/10.1007/s003740050426

Fontaine, S., Barot, S., Barré, P., Bdioui, N., Mary, B., & Rumpel, C. (2007). Stability of organic carbon in deep soil layers controlled by fresh carbon supply. *Nature*, 450(7167), 277–280. https://doi.org/10.1038/nature06275

Gatland, J. R., Santos, I. R., Maher, D. T., Duncan, T., & Erler, D. V. (2014). Carbon dioxide and methane emissions from an artificially drained coastal wetland during a flood: Implications for wetland global warming potential. *Journal of Geophysical Research: Biogeosciences*, 119(8), 1698–1716. https://doi.org/10.1002/2013JG002544

Glendell, M., Jones, R., Dungait, J., Meusburger, K., Schwendel, A., Barclay, R., Barker, S., Haley, S., Quine, T. A., & Meersmans, J. (2018). Tracing of particulate organic C sources across the terrestrial-aquatic continuum, a case study at the catchment scale (Carminowe Creek, Southwest England). *Science of the Total Environment*, 616, 1077–1088. https://doi.org/10.1016/j.scitotenv.2017.10.211

Graf-Rosenfellner, M., Cierjacks, A., Kleinschmit, B., & Lang, F. (2016). Soil formation and its implications for stabilization of soil organic matter in the riparian zone. *Catena*, 139, 9–18. https://doi.org/10.1016/j.catena.2015.11.010

Hinshaw, S., & Wohl, E. (2021). Quantitatively estimating carbon sequestration potential in soil and large wood in the context of river restoration. *Frontiers in Earth Science*, 9, 975. https://doi.org/10.3389/feart.2021.708895

Hooke, J. (1977). *An analysis of changes in River Channel patterns: The example of streams in Devon* (Doctoral dissertation, University of Exeter).

Hooke, J. M. (1980). Magnitude and distribution of rates of river bank erosion. *Earth surface processes*, 5(2), 143–157. https://doi.org/10.1002/esp.3760050205

Howard, A. D., & Knutson, T. R. (1984). Sufficient conditions for river meandering: A simulation approach. *Water Resources Research*, 20(11), 1659–1667. https://doi.org/10.1029/WR020i011p01659

Hupp, C. R., Kroes, D. E., Noe, G. B., Schenk, E. R., & Day, R. H. (2019). Sediment trapping and carbon sequestration in floodplains of the lower Atchafalaya Basin, LA: Allochthonous versus autochthonous carbon sources. *Journal of Geophysical Research: Biogeosciences*, 124(3), 663–677. https://doi.org/10.1029/2018JG004533

Isidorova, A., Mendonça, R., & Sobek, S. (2019). Reduced mineralization of terrestrial OC in anoxic sediment suggests enhanced burial efficiency in reservoirs compared to other depositional environments. *Journal of Geophysical Research: Biogeosciences*, 124(3), 678–688. https://doi.org/10.1029/2018JG004823

Johnson, S. 2018. Connecting the Culm. https://blackdownhillsaonb.org.uk/project/connecting-the-culm/

Lal, R. (2019). Accelerated soil erosion as a source of atmospheric CO2. *Soil and Tillage Research*, 188, 35–40. https://doi.org/10.1016/j.still.2018.02.001

Lambert, C., & Walling, D. (1987). Floodplain sedimentation: A preliminary investigation of contemporary deposition within the lower reaches of the river culm, Devon, UK. *Geografiska Annaler: Series A, Physical Geography*, 69(3–4), 393–404. https://doi.org/10.1080/04353676.1987.11880227

Lauer, J. W., & Parker, G. (2008). Modeling framework for sediment deposition, storage, and evacuation in the floodplain of a meandering river: Theory. *Water Resources Research*, 44(4), W04425. https://doi.org/10.1029/2006WR005528

Lewin, J., & Ashworth, P. J. (2014). The negative relief of large river floodplains. *Earth-Science Reviews*, 129, 1–23. https://doi.org/10.1016/j.earscirev.2013.10.014

Lewin, J., Ashworth, P. J., & Strick, R. J. (2017). Spillage sedimentation on large river floodplains. *Earth Surface Processes and Landforms*, 42(2), 290–305. https://doi.org/10.1002/esp.3996

Lewin, J., & Macklin, M. (2010). Floodplain catastrophes in the UKHolocene: Messages for managing climate change. *Hydrological Processes*, 24(20), 2900–2911. https://doi.org/10.1002/hyp.7704

Lininger, K. B., Wohl, E., & Rose, J. R. (2018). Geomorphic controls on floodplain soil organic carbon in the Yukon flats, interior Alaska, from reach to river basin scales. *Water Resources Research*, 54(3), 1934–1951. https://doi.org/10.1002/2017WR022042

Lugato, E., Smith, P., Borrelli, P., Panagos, P., Ballabio, C., Orgiazzi, A., Fernandez-Ugalde, O., Montanarella, L., & Jones, A. (2018). Soil erosion is unlikely to drive a future carbon sink in Europe. *Science Advances*, 4(11), eaau3523. https://doi.org/10.1126/sciadv.aau3523

Mayer, S., Schwindt, D., Steffens, M., Völkel, J., & Kögel-Knabner, I. (2018). Drivers of organic carbon allocation in a temperate slope-floodplain catena under agricultural use. *Geoderma*, 327, 63–72. https://doi.org/10.1016/j.geoderma.2018.04.021

Meersmans, J., Martin, M., Lacarce, E., Orton, T., de Baets, S., Gourrat, M., Saby, N. P. A., Wetterlind, J., Bispo, A., Quine, T. A., & Quine, T. A. (2013). Estimation of soil carbon input in France: An inverse modelling approach. *Pedosphere*, 23(4), 422–436. https://doi.org/10.1016/S1002-0160(13)60035-1

Moody, J. A., & Troutman, B. M. (2000). Quantitative model of the growth of floodplains by vertical accretion. *Earth Surface Processes and Landforms: The Journal of the British Geomorphological Research Group*, 25(2), 115–133. https://doi.org/10.1002/(SICI)1096-9837(200002)25:2<115::AID-ESP46>3.0.CO;2-Z

Nanson, G., & Croke, J. (1992). A genetic classification of floodplains. *Geomorphology*, 4(6), 459–486. https://doi.org/10.1016/0169-555X(92)90039-Q

Nanson, G. C. (1980). Point bar and floodplain formation of the meandering Beatton River, northeastern British Columbia, Canada. *Sedimentology*, 27(1), 3–29. https://doi.org/10.1111/j.1365-3091.1980.tb01155.x

Ni, J., Yue, Y., Borthwick, A. G., Li, T., Miao, C., & He, X. (2012). Erosion-induced CO2 flux of small watersheds. *Global and Planetary Change*, 94, 101–110. https://doi.org/10.1016/j.gloplacha.2012.07.003

Omengo, F. O., Geeraert, N., Bouillon, S., & Govers, G. (2016). Deposition and fate of organic carbon in floodplains along a tropical semiarid lowland river (Tana River, Kenya). *Journal of Geophysical Research: Biogeosciences*, 121(4), 1131–1143. https://doi.org/10.1002/2015JG003288

Pizzuto, J. E. (1987). Sediment diffusion during overbank flows. *Sedimentology*, 34(2), 301–317. https://doi.org/10.1111/j.1365-3091.1987.tb00779.x

[dataset] Quine, T., Cressey, E., Dungait, J., De Baets, S., Meersmans, J., Jones, M. W., & Nicholas, A. P. (2021). Geomorphically mediated carbon dynamics of floodplain soils and implications for net effect of carbon erosion. figshare. Dataset. 10.6084/m9.figshare.17263883.v1.

Quine, T. A., & Van Oost, K. (2007). Quantifying carbon sequestration as a result of soil erosion and deposition: Retrospective assessment using caesium-137 and carbon inventories. *Global Change Biology*, 13(12), 2610–2625. https://doi.org/10.1111/j.1365-2486.2007.01457.x

Raich, J. W., & Schlesinger, W. H. (1992). The global carbon dioxide flux in soil respiration and its relationship to vegetation and climate. *Tellus B*, 44(2), 81–99. https://doi.org/10.1034/j.1600-0889.1992.t01-1-00001.x

Regnier, P., Friedlingstein, P., Ciais, P., Mackenzie, F. T., Gruber, N., Janssens, I. A., Laruelle, G. G., Lauerwald, R., Luyssaert, S., Andersson, A. J., Arndt, S., Arnosti, C., Borges, A. V., Dale, A. W., Gallego-Sala, A., Goddéris, Y., Goossens, N., Hartmann, J., Heinze, C., … Andersson, A. J. (2013). Anthropogenic perturbation of the carbon

fluxes from land to ocean. *Nature Geoscience*, 6(8), 597–607. https://doi.org/10.1038/ngeo1830

Ricker, M. C., Donohue, S. W., Stolt, M. H., & Zavada, M. S. (2012). Development and application of multi-proxy indices of land use change for riparian soils in southern New England, USA. *Ecological Applications*, 22(2), 487–501. https://doi.org/10.1890/11-1640.1

Rosenbloom, N. A., Harden, J. W., Neff, J. C., & Schimel, D. S. (2006). Geomorphic control of landscape carbon accumulation. *Journal of geophysical research. Biogeosciences*, 111(G1), G01004. https://doi.org/10.1029/2005JG000077

Scheingross, J. S., Repasch, M. N., Hovius, N., Sachse, D., Lupker, M., Fuchs, M., Halevy, I., Gröcke, D. R., Golombek, N. Y., Haghipourd, N., Eglinton, T. I., Orfeo, O., Schleicher, A. M., & Haghipour, N. (2021). The fate of fluvially-deposited organic carbon during transient floodplain storage. *Earth and Planetary Science Letters*, 561, 116822. https://doi.org/10.1016/j.epsl.2021.116822

Schwendel, A. C., Nicholas, A. P., Aalto, R. E., Sambrook Smith, G. H., & Buckley, S. (2015). Interaction between meander dynamics and floodplain heterogeneity in a large tropical sand-bed river: The Rio Beni, Bolivian Amazon. *Earth Surface Processes and Landforms*, 40(15), 2026–2040. https://doi.org/10.1002/esp.3777

Six, J., Elliott, E., Paustian, K., & Doran, J. (1998). Aggregation and soil organic matter accumulation in cultivated and native grassland soils. *Soil Science Society of America Journal*, 62(5), 1367–1377. https://doi.org/10.2136/sssaj1998.03615995006200050032x

Sutfin, N. A., & Wohl, E. (2019). Elevational differences in hydrogeomorphic disturbance regime influence sediment residence times within mountain river corridors. *Nature Communications*, 10(1), 1–14. https://doi.org/10.1038/s41467-019-09864-w

Sutfin, N. A., Wohl, E., Fegel, T., Day, N., & Lynch, L. (2021). Logjams and channel morphology influence sediment storage, transformation of organic matter, and carbon storage within mountain stream corridors. *Water Resources Research*, 57, e2020WR028046. https://doi.org/10.1029/2020WR028046

Sutfin, N. A., Wohl, E. E., & Dwire, K. A. (2016). Banking carbon: A review of organic carbon storage and physical factors influencing retention in floodplains and riparian ecosystems. *Earth Surface Processes and Landforms*, 41(1), 38–60. https://doi.org/10.1002/esp.3857

Taillardat, P., Thompson, B. S., Garneau, M., Trottier, K., & Friess, D. A. (2020). Climate change mitigation potential of wetlands and the cost-effectiveness of their restoration. *Interface focus*, 10(5), 129. https://doi.org/10.1098/rsfs.2019.0129

Torres-Sallan, G., Schulte, R. P., Lanigan, G. J., Byrne, K. A., Reidy, B., Simó, I., Six, J., & Creamer, R. E. (2017). Clay illuviation provides a long-term sink for C sequestration in subsoils. *Scientific Reports*, 7(1), 1–7. https://doi.org/10.1038/srep45635

Van Oost, K., Verstraeten, G., Doetterl, S., Notebaert, B., Wiaux, F., Broothaerts, N., & Six, J. (2012). Legacy of human-induced C erosion and burial on soil–atmosphere C exchange. *Proceedings of the National Academy of Sciences*, 109(47), 19492–19497. https://doi.org/10.1073/pnas.1211162109

Walling, D. (2005). Tracing suspended sediment sources in catchments and river systems. *Science of the Total Environment*, 344(1–3), 159–184. https://doi.org/10.1016/j.scitotenv.2005.02.011

Walling, D., Fang, D., Nicholas, A., Sweet, R., Rowan, J., Duck, R., & Werritty, A. (2006). River flood plains as carbon sinks. *IAHS Publication*, 306, 460.

Walling, D. E., & Quine, T. (1990). Calibration of caesium-137 measurements to provide quantitative erosion rate data. *Land Degradation & Development*, 2(3), 161–175. https://doi.org/10.1002/ldr.3400020302

Wang, Z., Van Oost, K., Lang, A., Quine, T., Clymans, W., Merckx, R., Notebaert, B., & Govers, G. (2014). The fate of buried organic carbon in colluvial soils: A long-term perspective. *Biogeosciences*, 11(3), 873–883. https://doi.org/10.5194/bg-11-873-2014

Wiesmeier, M., Urbanski, L., Hobley, E., Lang, B., von Lützow, M., Marin-Spiotta, E., Wesemael, B., Rabot, E., Ließ, M., Garcia-Franco, N., Wollschläger, U., Vogel, H.-J., Kögel-Knabnerag, I., & Garcia-Franco, N. (2019). Soil organic carbon storage as a key function of soils-A review of drivers and indicators at various scales. *Geoderma*, 333, 149–162. https://doi.org/10.1016/j.geoderma.2018.07.026

Wohl, E., Castro, J., Cluer, B., Merritts, D., Powers, P., Staab, B., & Thorne, C. (2021). Rediscovering, reevaluating, and restoring lost river-wetland corridors. *Frontiers in Earth Science*, 9, 511. https://doi.org/10.3389/feart.2021.653623

Wohl, E., Hall, R. O., Jr., Lininger, K. B., Sutfin, N. A., & Walters, D. M. (2017). Carbon dynamics of river corridors and the effects of human alterations. *Ecological Monographs*, 87(3), 379–409. https://doi.org/10.1002/ecm.1261

Yan, P., Shi, P., Gao, S., Chen, L., Zhang, X., & Bai, L. (2002). 137Cs dating of lacustrine sediments and human impacts on Dalian Lake, Qinghai Province, China. *Catena*, 47(2), 91–99. https://doi.org/10.1016/S0341-8162(01)00193-X

Zimmermann, M., Leifeld, J., Schmidt, M., Smith, P., & Fuhrer, J. (2007). Measured soil organic matter fractions can be related to pools in the RothC model. *European Journal of Soil Science*, 58(3), 658–667. https://doi.org/10.1111/j.1365-2389.2006.00855.x

SUPPORTING INFORMATION

Additional supporting information can be found online in the Supporting Information section at the end of this article.